Fadlin_2022_IOP_Conf._Ser.__Earth_Environ._Sci._1117_012072.pdf

by

Submission date: 16-Jun-2023 08:03PM (UTC+0700)
Submission ID: 2117289322
File name: Fadlin_2022_IOP_Conf._Ser.__Earth_Environ._Sci._1117_012072.pdf (1.02M)
Word count: 3866
Character count: 20013

PAPER · OPEN ACCESS

Spatial Modelling for the Calculation of River Capacity: Case Study Downstream Area of Wanggu River Kendari

To cite this article: F Fadlin *et al* 2022 *IOP Conf. Ser.: Earth Environ. Sci.* **1117** 012072

View the article online for updates and enhancements.

You may also like

- Gravitational Collider Physics via ar–Black Hole Binaries
Qianhang Ding, Xi Tong and Yi Wang
- The Gemini/*HST* Galaxy Cluster Project: Environment Effects on the Stellar Populations in the Lynx Clusters at z = 1.27
Inger Jørgensen, Laura C. Hunter, Conor R. O'Neill et al.
- The Gemini/*HST* Galaxy Cluster Project: Redshift 0.2–1.0 Cluster Sample, X-Ray Data, and Optical Photometry Catalog
r Jørgensen, Kristin Chiboucas, Pascale Hibon et al.

This content was downloaded from IP address 182.1.169.114 on 14/06/2023 at 09:00

Spatial Modelling for the Calculation of River Capacity: Case Study Downstream Area of Wanggu River Kendari

F Fadlin[1]*, M A Thaha[2], F Maricar and M P Hatta[2]

[1]Doctoral Student of Civil Engineering Department, Hasanuddin University, Makassar, Indonesia
[2]Civil Engineering Department, Hasanuddin University, Makassar, Indonesia

*Corresponding author: ferifadlin@gmail.com

Abstract. Spatial modelling of flood-prone areas will provide maximum results if it is supported by the accuracy of the data acquired, mainly related to elevation data or the area's topography. Spatial modelling generated from accurate topographic data can estimate the river's carrying capacity. This study built a spatial model using data from aerial, terrestrial, and hydrographic surveys. Aerial surveys were conducted using UAV corrected by terrestrial surveys, GCP, and ICP. Testing the accuracy of the spatial model is carried out by comparing the results of current field velocity with the results of 2D Hec-Ras numerical simulations using a variation of the manning coefficient. The combination of aerial, terrestrial, and hydrographic surveys produces a cross-sectional spatial model of the river, which is used in calculating the river's carrying capacity. The river's capacity is calculated using a 2D numerical simulation method using Hec-Ras software and verified by a mathematical approach based on the flood hydrograph curve. The results showed that the horizontal accuracy of the GCP was 2.8 cm and the vertical accuracy was 6.5 cm. The results of testing the vertical elevation accuracy of aerial photographs on terrestrial topographic data measured in the field (ICP) have a Mean Absolute Percentage Error (MAPE) value of 5.81%. According to the spatial model, the manning roughness value is 0.06-0.09. The river's capacity based on numerical simulations is 1.700.766 m3, and the results of the verification using a mathematical approach are 1.683.433 m^3 with a difference of 1.02%.

Introduction

One of the problems faced by the government of Kendari City in reducing the risk of flood disasters is the lack of spatial information about the condition of the area that has the potential to be affected by flooding, which can cause material and non-material losses. The unavailability of this information can exacerbate the losses incurred if this flood disaster occurs in the future. The next problem occurs in the managerial aspect, namely the stakeholders or agencies that have duties and functions in flood control. The problem is that the supporting data in controlling the destructive power of water or flooding are not integrated, so it is difficult to control. The impact of these problems is the determination of policies for the direction of the flood control program, including aspects of budgeting that become inappropriate due to inaccuracies in data and information. Policies that are constantly changing and the absence of a track record of data make the proposed activities in flood control unstructured and unintegrated.

Spatial modelling of flood-prone areas will provide maximum results if it is supported by the accuracy of the data acquired, mainly related to elevation data or the site's topography [1]. The extraction of altitude data to obtain a map of the regional situation can be earned using various methods or

Content from this work may be used under the terms of the Creative Commons Attribution 3.0 licence. Any further distribution of this work must maintain attribution to the author(s) and the title of the work, journal citation and DOI.
Published under licence by IOP Publishing Ltd

approaches, such as direct surveys or secondary data from satellite imagery with Digital Elevation Model (DEM) radar technology. These different methods have their respective advantages and disadvantages. DEM satellite images and topographic maps from Indonesian Geospatial Agency RBI maps are accessible data sources for a wide area. The data's weakness is the accuracy level. The RBI map provides data with a full scale currently available of 1:50.000 and DEM satellite imagery with a maximum spatial resolution of 0.27 arc second or about 8,3 meters. Field surveys can be carried out using measuring equipment (Total Station) with a relatively high level of accuracy if carried out with the correct method and high expertise from the surveyor. Still, it requires time and effort and also higher costs. The last method that can be used and is currently significantly developed in mapping the area is unmanned aircraft or Unmanned Aerial Vehicles (UAV) [2]. The use of UAV can provide information on the condition or situation of a site in great detail with a very high spatial resolution and can cover a large area in a shorter time [3]. The weakness of the UAV is that the acquired elevation data is Digital Surface Model (DSM) data or surface elevation features. To improve the accuracy of UAV acquisition data, DSM can be derived into Digital Terrain Model (DTM) using Bench Mark (BM) as the ground control point (GCP).

Research on spatial flood modelling has been carried out in various cities worldwide. One of the studies was conducted to prepare hydrodynamic models and flood inundation mapping using the Geographic Information System method [4]. The unit of analysis used in the research is the river using echosounder equipment for river bathymetry mapping. The resulting research output is an integrated terrain model between land topography data (DEM spatial resolution of 30 meters) and river bathymetry for flood inundation modelling. The combination of remote sensing methods and Geographic Information Systems (GIS) is also used to map flood risk downstream of the Togo River, West Africa [5]. The unit of analysis used is Watershed, with the main output being a flood risk map. In 2018 research on flood risk assessment using LiDAR technology was carried out using administrative areas as the unit of analysis [6]. The main output target of this study is to increase the accuracy of the primary data used in making flood inundation models. LIDAR technology is one of the topographic data acquisition technologies currently developing but requires very high costs in its utilization, so it isn't easy to use. Based on previous studies and literature reviews, the researchers intend to assess the risk of flooding using a photogrammetric approach using UAV technology data to compile a spatial model of the river. Flood tracking data and bathymetry information are collected in a spatial model of flood inundation simulation as the basis for compiling a flood risk map in Kendari City, where the initial study is to develop a spatial model for the downstream area for the calculation of river capacity.

2. Method

2.1. Location

This research was carried out in Kendari City in flood-affected areas in 2013/ 2017, namely downstream of the Wanggu river. The determination of the boundaries of the study area is carried out based on historical data on flood events at the research location. The research location can be seen in Figure 1.

Figure 1. Research location

2.2. *Terrestrial Survey*

The Global Navigation Satellite System (GNSS) survey was conducted to obtain the coordinates of the Ground Control Point (GCP) for aerial photo correction, bathymetric and tidal measurement benchmarks. In general, 2 GNSS survey methods can be used, namely Real Time Kinematic (RTK) and Static methods. In principle, the measurement procedure uses a benchmark that has coordinates as a base and a location benchmark whose coordinates will be known as a rover. The command used in this study is the CORS (Continuously Operating Reference Stations) station and several stations of the nearest geodetic control point as an alternative.

2.3. *Aerial Survey*

The stages in mapping river landscapes using UAV technology are divided into 5: the initial survey of the location, pre-flight field work for GCP installation and UAV vehicle testing, UAV flight missions, quality check, data processing, and data extraction.

1. Initial Survey Map Site; This stage is the initial or preparation stage before data collection is carried out. The most critical aspects that must be carried out at this stage are identifying obstacles (obstacle identification), determining the position of the take-off and landing point, and designing the flight path. The trials included administrative practices, licensing arrangements, and the preparation of equipment and materials used in data collection.
2. Pre-flight fieldwork; The initial survey of the site map results is used to identify the Ground Control Point installation point (GCP) as the control point for developing orthomosaic photos. The GCP is installed on the flight path traversed by the UAV and avoids obstacles so that it is easily observed during the geometric correction of aerial photographs. Installation of GCP control points using the Global Navigation Satellite System (GNSS survey approach with the Real Time Kinematic GPS (RTK-GPS) method by taking the base at the nearest geodetic control network point from the research location (maximum distance of 2 km). The RTK-GPS method was chosen because it has a position accuracy level ranging from centimetres to decimeters [7]. At this stage, a UAV readiness check is also carried out, which includes flight altitude and camera settings.
3. Flight missions; The flight mission is carried out in several stages based on the design results (flight plan) on the Drone Deploy application. The UAV vehicle used in this mission is the DJI Mavic 2 Pro, with a maximum flight duration of 30 minutes at a safe distance of 500 meters.
4. Data Processing and Quality Check. Data processing and quality checks were carried out using ArcgisPro software. Data processing begins with flight path reconstruction, photo compilation, Ground Control Point correction, dense point cloud construction, and creating DEM and orthophoto.
5. Data Extraction. The data extracted from the results of data processing consists of raster data (aerial photos in tif and DEM format) and vector data in the form of points, lines, polygons, and objects. The data is then used as input in preparing the calculation of river capacity.

2.4. *Hydrographic Survey*

A hydrographic survey collects hydrographic information, including depth, currents, sediments, tides, and details of the situation and shoreline. The generalization begins with determining the boundaries of the area to be measured, preparing the route, preparing tools and vehicles (ships), and measuring tides. In general, the stages of this activity can be seen in Figure 2. In this study, the hydrographic survey focused on measuring the depth of the river and the tides, which also affect the water level in the river.

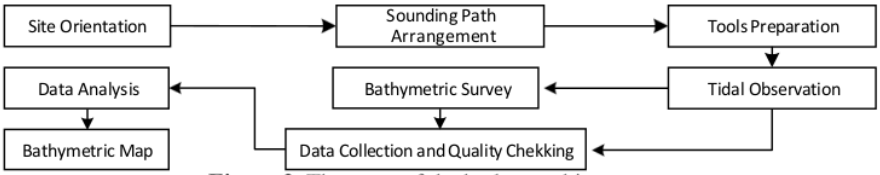

Figure 2. The steps of the hydrographic survey

3. Result and Discussion

The terrain model is a spatial model as the primary data used in calculating river capacity and flood simulations as a basis for determining flood hazards [8]. The terrain model in this study was compiled using data from aerial photo surveys, river bathymetry surveys, and terrestrial surveys/ topographic measurements directly in the field at several points. The topographic data generated from the processing of aerial photographs is then combined with bathymetric data and tested for accuracy using a sample of data from direct measurements in the field called the Independent Control Point (ICP). The graph of filed information, distribution of ICP points, and comparison of data between ICP and the result of aerial photos can be seen in Figure 3.

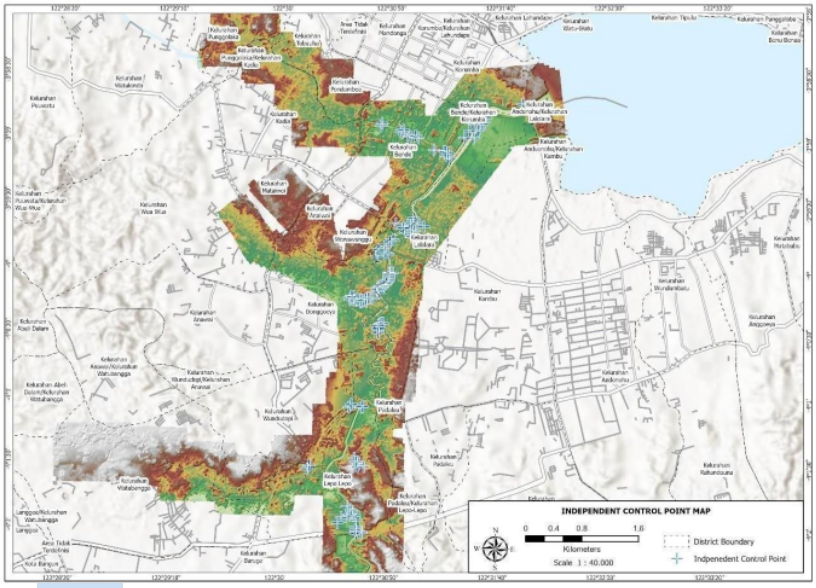

Figure 3. Terrain Model and The Distribution of Independent Control Point

Based on the Digital Surface Model (DSM) accuracy test of the downstream elevation, the average error data from aerial photography is 0,18 meters or 18 cm, and the mean absolute percentage error (MAPE) is 5.81 %. MAPE provides information on how significant the error value of the simulation data is to the measured data in the field [9]. The range of values used is the model's ability, or the prediction results are excellent if the MAPE value is less than 10 %, while the forecasting model is bad if the MAPE value is greater than 50%. Based on the data analysis, the Mean Absolute Percentage Error of terrain model elevation is 5.81% (Very Good). The comparison of field elevation data and terrain model can be seen in figure 4.

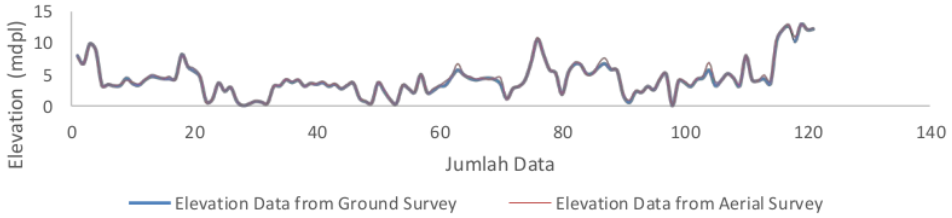

Figure 4. Comparison of Elevation Data from Aerial Photos and Field Data

The river cross-section spatial model data is then used to analyze and determine the volume of the downstream capacity of the Wanggu River. The capacity analysis is carried out by 2D Numerical simulation using Hec-Ras. Hec-Ras is one hydraulic model used widely in simulating flow patterns on the river [10]. Before carrying out the capacity analysis, the first step is to validate the simulation model to determine the appropriate computational grid size and the manning roughness coefficient according to the conditions in the field. The input data used is a cross-sectional spatial model of the river as a terrain model, upstream flow/discharge (Q25), and stage hydrograph using tidal data from secondary data. Data validation is carried out using the results of current velocity measurements at several measurement points. The current velocity measurement data is also used to determine the manning roughness coefficient at the bottom of the Wanggu River. The simulation scheme can be seen in Figure 1.

The type of riverbed at the research site is muddy soil. Based on the roughness table of the manning roughness coefficient data from the literature study results, the range of manning values for soil channels is 0.016 to 0.14. The selection of the value range was also based on the riverbed characteristics obtained from the bathymetric measurements using deeper sonar (Figure 5). Orange colour indicates the primary type of complex (hardest) channel in the form of subgrade, brown (medium), and black (smoothest). The green layer indicates the reflection of sonar waves with a weak signal indicating an organic layer above the surface of the riverbed. The simulation is carried out by inputting the discharge at the inflow and the tide at the outflow points. The results of the discharge measurement at the simulation input location can be seen in Figure 6. At the time of measuring the condition of the Kendari Bay waters towards high tide, the sea level elevation was at a position of 0.8 – 1.06 mdpl, and the measured discharge at the inflow point was 16,176 m3/s.

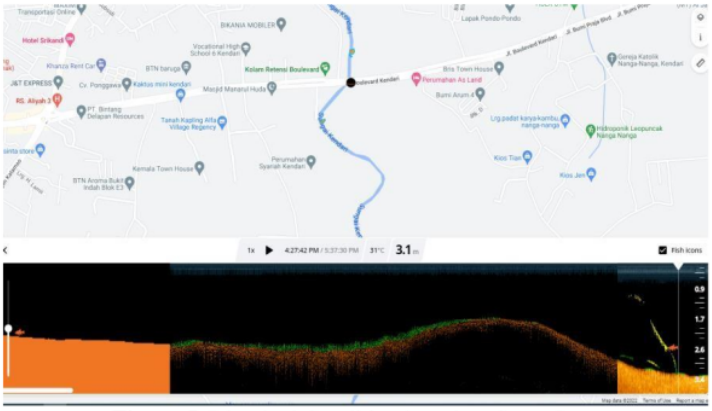

Figure 5. Riverbed Condition based on Sonar Data

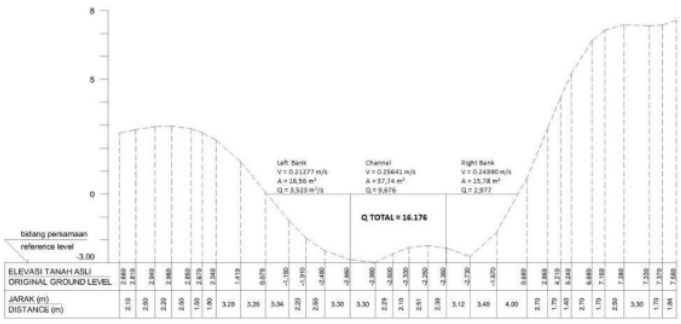

Figure 6. Cross Section at Upstream Boundary Condition Line

Validation is done by comparing the flow velocity of the measurement results in the field with the flow velocity of the simulation results at Point I and Point II. Model validation was also carried out using data from measurements in the area and evaluated using the Mean Absolute Percentage Error approach. In verifying the model, the manning roughness coefficient was also analyzed to determine the most suitable range of manning roughness for use in 2D flow simulations downstream of the Wanggu River, Kendari City. A comparison of flow velocity results from simulation and field measurements in several ranges of manning values (n = 0.01 – 0.14) can be seen in Figure 7.

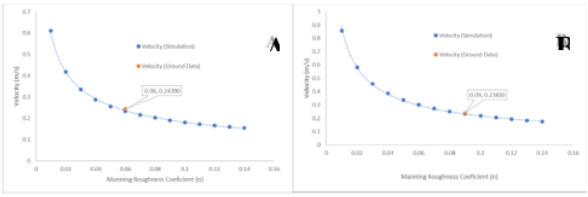

Figure 7. Comparison of Flow Velocity Simulation Results and Field Measurements in the Range n 0.01 – 0.14 Validation Points I (A) and II (B)

Based on the graph, it can be seen that at validation point I, the flow velocity of the field measurement results of 0.243 m/s has a comparable value to the simulation results using a manning coefficient of 0.06 with a Mean Absolute Percentage Error (MAPE) of 4.46%. Meanwhile, at validation point II, the flow velocity of the field measurement results has a value with the simulation results at 0.09 manning coefficient with a MAPE value of 2.56%. The data from the simulation shows that the spatial model of the downstream area of the Wanggu River resulting from aerial photography, topographic surveys, and bathymetry has a manning coefficient value range between 0.06 – 0.09. The spatial model that has been validated is then used in simulations to determine the downstream capacity of the Wanggu river. The flood discharge used is the flood discharge for 25 years in the Upper Wanggu Sub-watershed and tidal data in the downstream area. The determination of the carrying capacity is based on the simulation time, which shows an overflow in the river at 2 hours 45 minutes after the flow of the flood discharge at the 25-year return period. Based on the simulations, the river overflows when the upstream burst reaches 435,271 m^3/s, and the recorded volume accumulation in the downstream area is 1,700,766 m^3. Based on these data, it can be concluded that the maximum capacity of the downstream region of the Wanggu River is 1,700,766 m^3. In addition to the simulation method, the calculation of the river's carrying capacity is also carried out using a mathematical approach using a 25-year flood hydrograph curve graph used as input for simulation data, which can be seen in Figure 8.

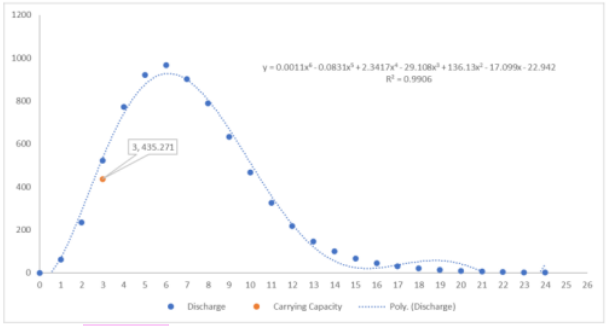

Figure 8. 25-year Return Periode Hydrograph

Based on the figure, it can be seen that the hydrograph curve approaches the polynomial equation pattern $y = 0.0011x^6 - 0.0831x^5 + 2.3417x^4 - 29.108x^3 + 136.13x^2 - 17.099x - 22.942$ f(x) with a coefficient of determination $R^2 = 99.06\%$ where the x-axis is time (t) and y-axis is discharged. From the simulation results, there was an overflow in the river when the discharge reached 435.271 (y = 435.271),

precisely at the 2nd hour over 45 minutes (2.75 hours) which can be seen in the formula below. Calculate the volume of the river's capacity. It can be done by integrating the equation of the curve function concerning time on the X axis and then converting it to seconds and reducing the function at the maximum discharge during a flood event. The equations in calculating the volume of the downstream capacity of the Wanggu River are:

$$\int_{t_0}^{t_{overflow}} (f(x) - g(x) \, \partial x \quad (1)$$

Based on the calculations using the above equation, the downstream capacity of the Wanggu River is 1,683,433 m^3. Compared with the simulation data, there is a difference of 17,333 m^3 or 1.02%. Based on the results of the simulation and mathematical analysis, it can be concluded that the downstream capacity of the Wanggu River is in the range of 1,683,433 - 1,700,766 m^3.

4. Conclusion

The results showed that the horizontal accuracy of the GCP was 2.8 cm and the vertical accuracy was 6.5 cm. The results of testing the vertical elevation accuracy of aerial photographs on terrestrial topographic data measured in the field (ICP) have a Mean Absolute Percentage Error (MAPE) value of 5.81%. The manning roughness value of the spatial model is 0,06 -0,09. The river's capacity based on numerical simulations is 1.700.766 m^3, and the results of the verification using a mathematical approach are 1.683.433 m3 with a difference of 1.02%.

REFERENCES

[1] D. Molinari *et al*., "Validation of flood risk models : current practice and possible improvements," *Int. J. Disaster Risk Reduct*., 2018, doi: 10.1016/j.ijdrr.2018.10.022.

[2] M. La Salandra *et al*., "Generating UAV high-resolution topographic data within a FOSS photogrammetric workflow using high-performance computing clusters," *Int. J. Appl. Earth Obs. Geoinf*., **vol. 105**, no. June, p. 102600, 2021, doi: 10.1016/j.jag.2021.102600.

[3] Y. Watanabe and Y. Kawahara, "UAV Photogrammetry for Monitoring Changes in River Topography and Vegetation," *Procedia Eng*., **vol. 154**, pp. 317–325, 2016, doi: 10.1016/j.proeng.2016.07.482.

[4] S. Saksena, V. Merwade, and P. J. Singhofen, "Flood inundation modelling and mapping by integrating surface and subsurface hydrology with river hydrodynamics," *J. Hydrol*., **vol. 575**, no. June, pp. 1155–1177, 2019, doi: 10.1016/j.jhydrol.2019.06.024.

[5] J. Ntajal, B. L. Lamptey, B. Ibrahim, and B. K. Nyarko, "Flood Disaster Risk Mapping in the Lower Mono River Basin in Togo, West Africa," *Int. J. Disaster Risk Reduct*., 2017, doi: 10.1016/j.ijdrr.2017.03.015.

[6] M. Rusnák, J. Sládek, A. Kidová, and M. Lehotský, "Template for high-resolution river landscape mapping using UAV," *Measurement*, 2017.

[7] S. Hemmelder, W. Marra, H. Markies, and S. M. De Jong, "Monitoring river morphology & bank erosion using UAV imagery – A case study of the river Buëch, Hautes-Alpes, France," *Int J Appl Earth Obs Geoinf*., **vol. 73**, no. April, pp. 428–437, 2018, doi: 10.1016/j.jag.2018.07.016.

[8] C. Ben Khalfallah and S. Saidi, "Spatiotemporal floodplain mapping and prediction using HEC-RAS - GIS tools : Case of the Mejerda river, Tunisia," *J. African Earth Sci*., **vol. 142**, pp. 44–51, 2018, doi: 10.1016/j.jafrearsci.2018.03.004.

[9] U. Khair, H. Fahmi, S. Al-Hakim, and R. Rahim, "Forecasting Error Calculation with Mean Absolute Deviation and Mean Absolute Percentage Error," *J. Phys. Conf. Ser*., vol. 930, no. 1, 2017, doi: 10.1088/1742-6596/930/1/012002.

[10] R. Maatta, P. K. Joshi, and A. K. Jindal, "Solar power potential mapping in India using remote sensing inputs and environmental parameters," *Renew. Energy*, **vol. 71**, pp. 255–262, 2014, doi: 10.1016/j.renene.2014.05.037.

Fadlin_2022_IOP_Conf._Ser.__Earth_Environ._Sci._1117_0120...

ORIGINALITY REPORT

13%	9%	7%	7%
SIMILARITY INDEX	INTERNET SOURCES	PUBLICATIONS	STUDENT PAPERS

PRIMARY SOURCES

1	Submitted to University of Greenwich Student Paper	2%
2	ijettjournal.org Internet Source	2%
3	istina.ipmnet.ru Internet Source	2%
4	core.ac.uk Internet Source	1%
5	academic.oup.com Internet Source	1%
6	pertambangan.fst.uinjkt.ac.id Internet Source	1%
7	Submitted to Higher Education Commission Pakistan Student Paper	<1%
8	Submitted to Politeknik Negeri Sriwijaya Student Paper	<1%
9	eprints.uad.ac.id Internet Source	<1%

10	C Kara Mostefa Khelil, B Amrouche, K Kara. "Fault detection and diagnosis of GCPV systems using bayesian neural network", Journal of Physics: Conference Series, 2022 Publication	<1 %
11	www.uetpeshawar.edu.pk Internet Source	<1 %
12	Ahmad Yanie, Abdurrozaq Hasibuan, I Ishak, M Marsono et al. "Web Based Application for Decision Support System with ELECTRE Method", Journal of Physics: Conference Series, 2018 Publication	<1 %
13	Huanhuan Wang, Dan Yakir, Eyal Rotenberg. "Assessing the effectiveness of a central flux tower in representing the spatial variations in gross primary productivity in a semi-arid pine forest", Agricultural and Forest Meteorology, 2023 Publication	<1 %
14	iopscience.iop.org Internet Source	<1 %
15	repository.unej.ac.id Internet Source	<1 %
16	Yi Wang, Mingyuan He, Jie Xiang, Jingjing Ge. "Block Adjustment of Large-scale Domestic Optical Satellite Remote Sensing Imagery	<1 %

without GCP in Antarctic", IOP Conference Series: Earth and Environmental Science, 2020
Publication

Exclude quotes	On	Exclude matches	< 5 words
Exclude bibliography	On		